

Facile and green decoration of Pd nanoparticles on macroporous carbon by polyoxometalate with enhanced electrocatalytic ability

Yufan Zhang*, Huan Wang, Qianqian Yao, Fei Yan, Chunyan Cui, Mengyuan Sun
and Hongyi Zhang*

Key Laboratory of Analytical Science and Technology of Hebei Province, College of Chemistry and Environmental Science, Key Laboratory of Medicinal Chemistry and Molecular Diagnosis, Ministry of Education, Hebei University, 071002 Baoding, P R China

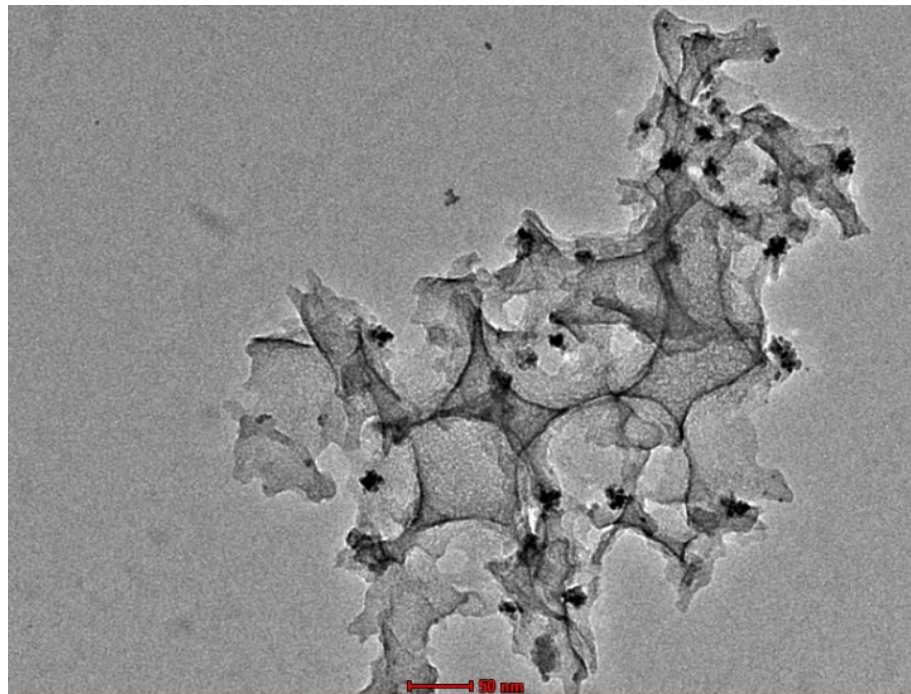


Fig. S1 TEM image of Pd@POMs/MPC-3.

* Corresponding author: Tel.: +86 0312 5079403; Fax: +86 0312 5079403.

E-mail address: zyf@hbu.edu.cn (Y.F. Zhang). hyzhang@hbu.edu.cn (H.Y. Zhang)

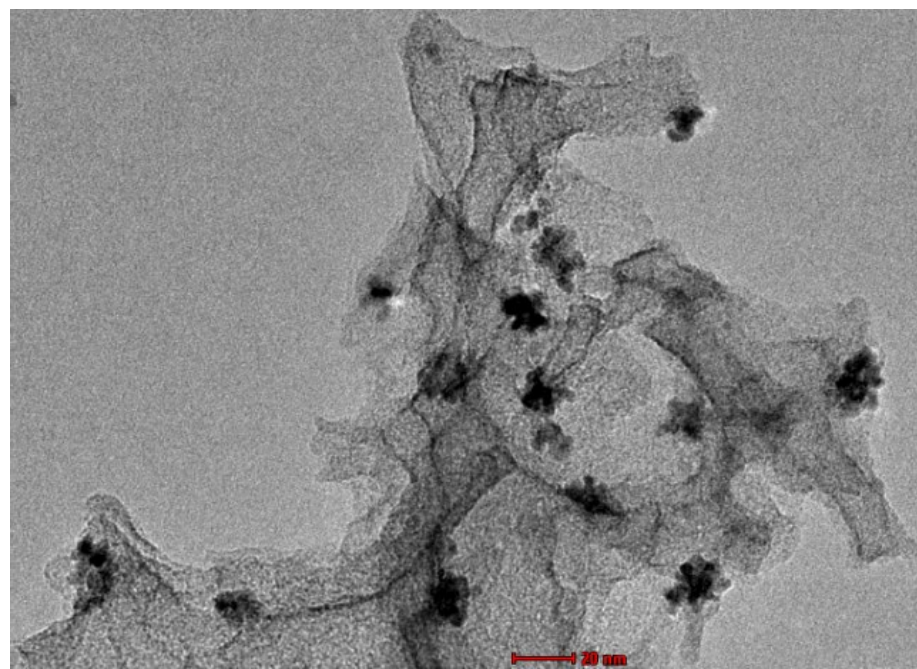


Fig. S2 TEM image of Pd@POMs/MPC-3.

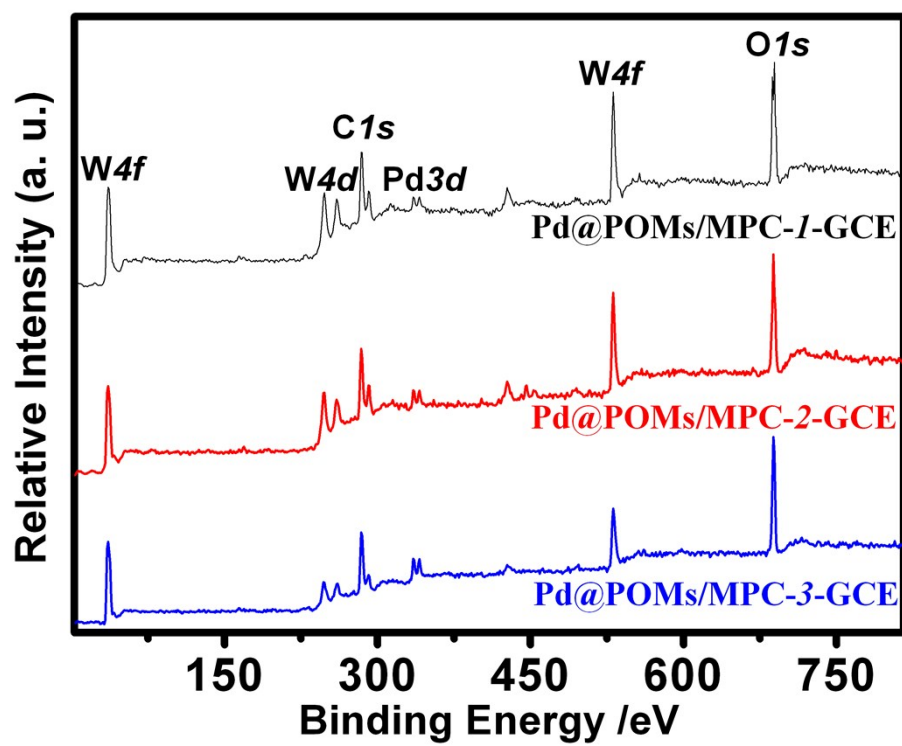


Fig. S3 The wide survey spectra of Pd@POMs/MPC-1, 2, and 3.

Table S1 Elemental composition of Pd@POMs/MPC-1, 2, and 3

Samples	XPS (at %)			
	C	Pd	W	O
Pd@POMs/MPC-1	71.26	0.23	2.56	25.95
Pd@POMs/MPC-2	70.23	0.86	3.87	25.04
Pd@POMs/MPC-3	69.89	2.32	4.16	23.63

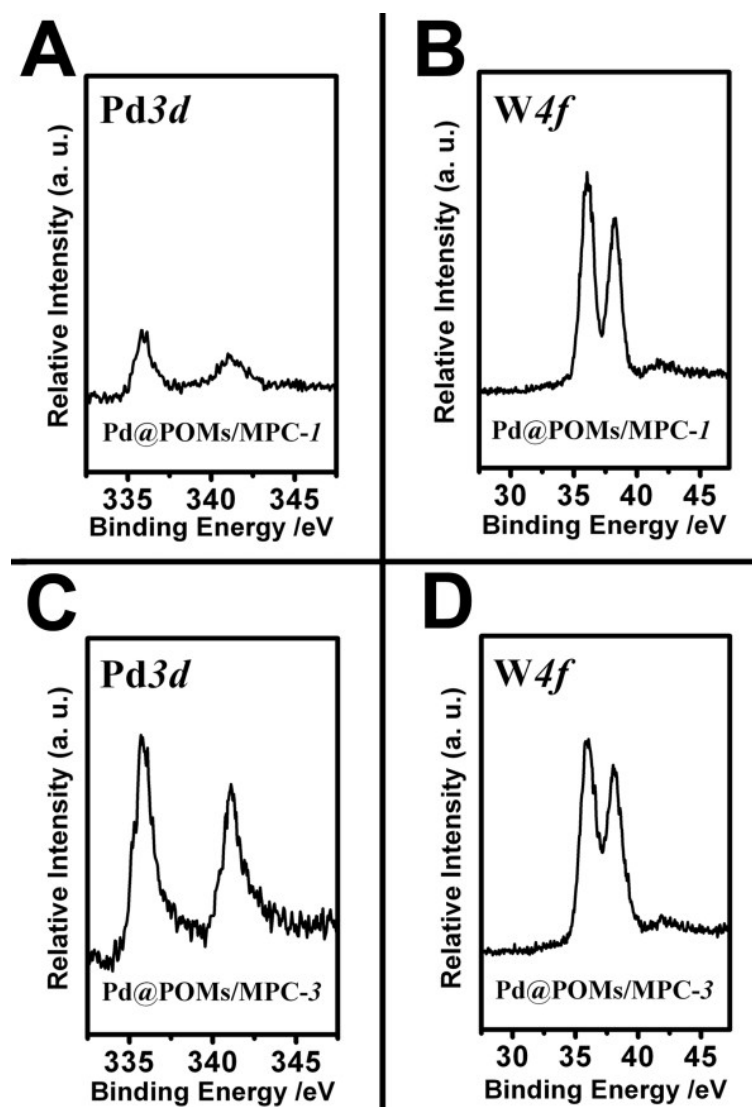


Fig. S4 XPS spectra of the Pd 3d and W 4f in the Pd@POMs/MPC-1 and -3 nanohybrids.

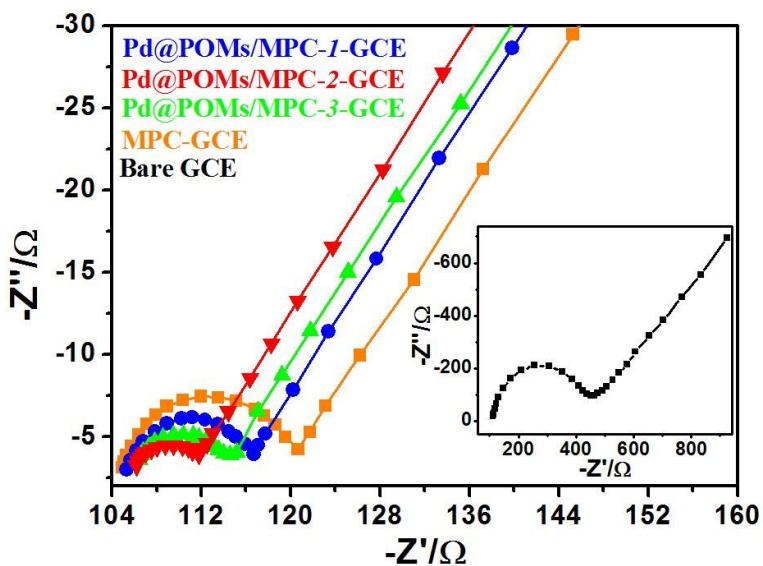


Fig. S5 EIS of as-prepared products in a 0.1 M KCl solution containing 5.0 mM $\text{K}_3\text{Fe}(\text{CN})_6$ – $\text{K}_4\text{Fe}(\text{CN})_6$ and from 0.1 Hz to 10.0 KHz (A).

Table S2 Comparison of the R_{ct} and responses of different electrodes towards to $\text{K}_3\text{Fe}(\text{CN})_6/\text{K}_4\text{Fe}(\text{CN})_6$ (for five determinations)

Electrode	bare GCE	MPC-GCE	Pd@POMs/MPC-1-GCE	Pd@POMs/MPC-2-GCE	Pd@POMs/MPC-3-GCE
R_{ct} (Ω)	345.31	16.08	11.36	6.18	9.03

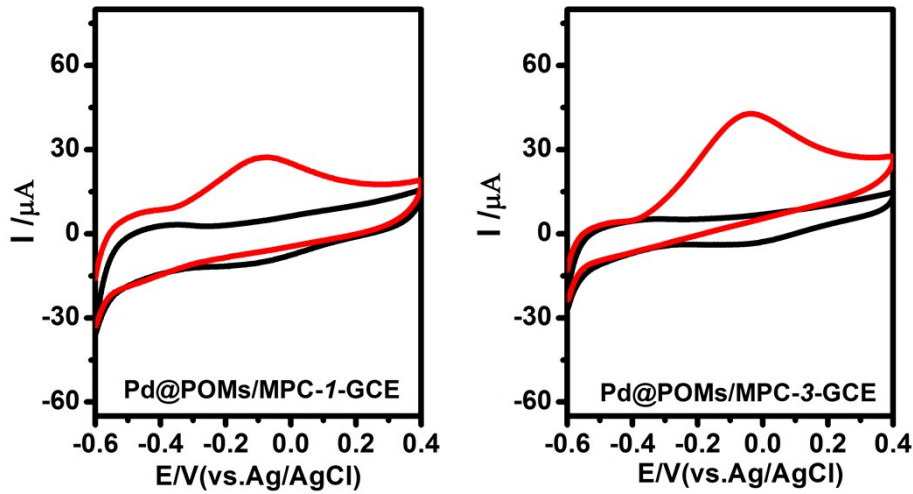


Fig. S6 CVs of Pd@POMs/MPC-1-GCE and Pd@POMs/MPC-3-GCE in the absence (black line)

and presence (red line) of 100 μM hydrazine (pH=7.0). Scan rate: 50 mV s^{-1} .

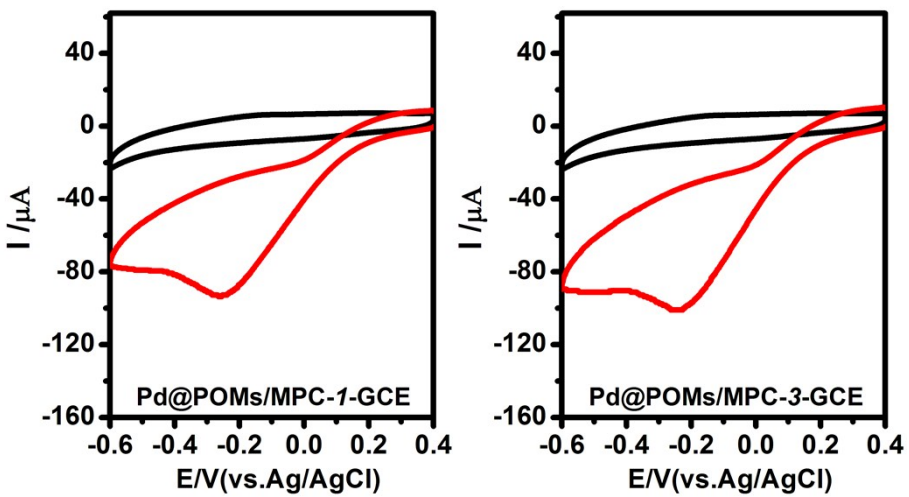


Fig. S7 CVs of Pd@POMs/MPC-1-GCE and Pd@POMs/MPC-3-GCE in the absence (black line) and presence (red line) of 1.0 mM H_2O_2 ($\text{pH}=7.0$). Scan rate: 50 mV s^{-1} .

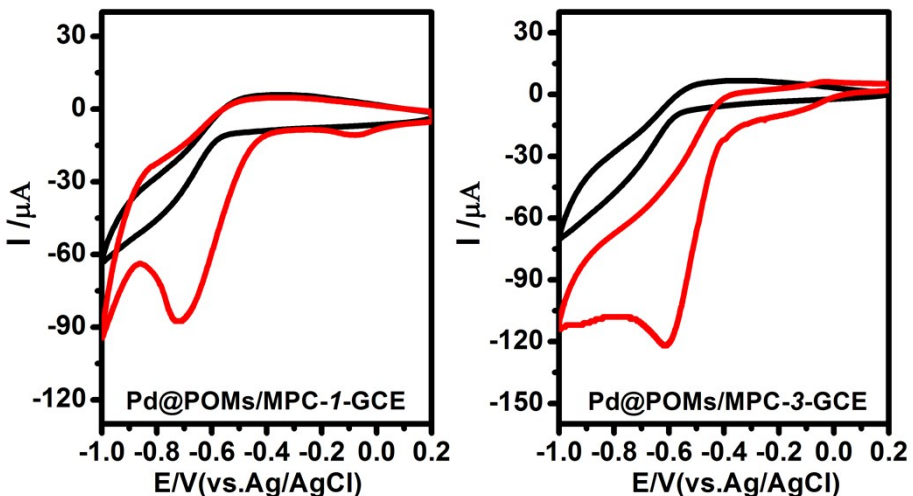


Fig. S8 CVs of Pd@POMs/MPC-1-GCE and Pd@POMs/MPC-3-GCE in the absence (black line) and presence (red line) of $100 \mu\text{M}$ NB ($\text{pH}=7.0$). Scan rate: 50 mV s^{-1} .

Table S3 Comparison of the performance of the Pd@POMs/MPC-2–GCE for the electrochemical detection of hydrazine with that of other modified electrodes.

Working electrode	potential (V)	Linear range (μM)	sensitivity ($\mu\text{A mM}^{-1}$)	Limit of detection (μM)	Response time (s)	Reference
RGO/ZnO–Au/GCE ^a	0.1 (Ag/AgCl)	0.05-5	393.34	0.018	3	1
PA6/PANI_ZnO/FTO ^b	0.19 (Ag/AgCl)	0.5-5000	61.77	0.35	-	2
Ag/ZIF-8/CPE ^c	-0.05 (Ag/AgCl)	6-5000	3.87	1.57	3	3
Co ₃ O ₄ NWs/GCE ^d	0.5 (Ag/AgCl)	20-700	28.63	0.5	-	4
Nafion–TiO ₂ –CNT/GCE ^e	0.4 (Ag/AgCl)	0.35-162	58	0.22	5	5
rGO–PxDA–Pd/GCE ^f	0.1 (Ag/AgCl)	1-7433	15.2	0.17	3	6
Co ₃ O ₄ /MWCNTs/GCE ^g	0.5 (SCE ^l)	20-1100	34.5	0.8	5	7
Pt–Cu@PSi/CILE ^h	0 (Ag/AgCl)	0.2-1680	10.35	0.05	-	8
PNi-TPPS ₄ -NPs/GCE ⁱ	0.55 (Ag/AgCl)	1-400	0.99	0.11	-	9
Au/PDTYB/MWCNTs/GCE ^j	0.08 (Ag/AgCl)	2-350	41.63	0.6	-	10
PB@Ag/GF ^k	0.3 (Ag/AgCl)	0.5-8.5	26.06	0.49	2	11
Pd@POMs/MPC-2–GCE	0 (Ag/AgCl)	2-2450	62.8	0.82	4	This work

a Reduced graphene oxide nanosheets/ZnO microspheres–Au nanoparticles modified glassy carbon electrode

b Polyamide 6/polyaniline (PA6/PANI) electrospun nanofibers decorated with ZnO nanoparticles modified fluorine doped tin oxide electrode

c Ag/zeolitic imidazolate frameworks nanocomposite modified glassy carbon electrode

d Porous Co₃O₄ nanowire modified glassy carbon electrode

e Nafion–coated titanium oxide nanoparticle deposition on carbon nanotube surfaces modified glassy carbon electrode

f Graphene functionalized by benzylamine molecules and subsequently palladium modified glassy carbon electrode

g Co₃O₄ nanoparticles decorated on the multi-walled carbon nanotubes modified glassy carbon electrode

h Pt–Cu nanoalloy was supported on the surface of porous silicon modified carbon ionic liquid electrode

i Poly-(5, 10, 15, 20-tetra (4-sulfophenyl) porphyrin–nickel)modified glassy carbon electrode

j Poly (4, 5-dihydro-1, 3-thiazol-2-ylsulfanyl-3-methyl-1, 2-benzenediol)–gold nanoparticles film on multi-walled carbon nanotubes modified glassy carbon electrode

k Prussian blue/silver nanoparticles modified freestanding graphite felt

l Saturated calomel electrode

Table S4 Comparison of the performance of the Pd@POMs/MPC-2–GCE for the electrochemical detection of H₂O₂ with that of other modified electrodes.

Working electrode	potential (V)	Linear range (μM)	sensitivity ($\mu\text{A mM}^{-1}$)	Limit of detection (μM)	Response time (s)	Reference
Cu/PSi/CPE ^a	-0.2 (Ag/AgCl)	0.5-3780	13.09	0.27	5	12
NP–PtAu/GCE ^b	0.7 (RHE ^l)	50-2750	1.43	0.1	-	13
P _p PDA@Fe ₃ O ₄ /GCE ^c	-0.4 (SCE ^m)	0.5-400	76	0.21	-	14
GF/Co ₃ O ₄ –NP/GCE ^d	-0.48 (Ag/AgCl)	0.2-211.5	90.97	0.06	10	15
TOAB/ZnPp–C ₆₀ /GCE ^e	-1.17 (Ag/AgCl)	35-3400	215.6	0.81	2	16
HRP/C–Dots/LDHs/GCE ^f	-0.35 (SCE)	0.1-23.1	37.51	0.04	-	17
Pt/PG/GCE ^g	0.14 (Ag/AgCl)	1-1477	27.22	0.5	3	18
Au NPs–N–GQDs/GCE ^h	-0.4 (Ag/AgCl)	0.25-13327	14.86	0.12	5	19
PPy–Pt/GCE ⁱ	-0.175 (Ag/AgCl)	500-6300	13.16	0.6	-	20
graphene/pectin–CuNPs/GCE ^j	-0.24 (Ag/AgCl)	1-1000	31.20	0.35	-	21
Pt–MnO _x @C/GCE ^k	0.4 (Ag/AgCl)	2-4000	9.81	0.7	-	22
Pd@POMs/MPC-2–GCE	-0.17 (Ag/AgCl)	1-110 110-1710	98.5 76.2	0.36	2	This work

a Copper on porous silicon nanocomposite modified carbon paste electrode

b Nanoporous Pt–Au alloy modified glassy carbon electrode

c Poly(*p*-phenylenediamine) (P_pPDA)–Fe₃O₄ nanocomposite modified glassy carbon electrode

d Graphene and cobalt oxide nanoparticles composite modified glassy carbon electrode

e Zinc porphyrin–fullerene was entrapped in tetraoctylammonium bromide film modified glassy carbon electrode

f Carbon nanodots and CoFe layered double hydroxide composites modified glassy carbon electrode

g Pt nanoparticles decorated porous graphene nanocomposite modified glassy carbon electrode

h Au nanoparticles on nitrogen–doped graphene quantum dots modified glassy carbon electrode

i Polypyrrole/platinum nanocomposite modified glassy carbon electrode

j Graphene/pectin/copper nanoparticles modified glassy carbon electrode

k carbon supported Pt–MnO_x nanoparticles modified glassy carbon electrode

l Reversible hydrogen electrode

m Saturated calomel electrode

Table S5 Comparison of the performance of the Pd@POMs/MPC-2–GCE for the electrochemical detection of NB with that of other modified electrodes.

Working electrode	potential (V)	Linear range (μM)	sensitivity ($\mu\text{A mM}^{-1}$)	Limit of detection (μM)	Reference
RGO–AgNPs/GCE ^a	-0.45 (Ag/AgCl)	0.5–900	59.36	0.26	23
Pd–GG–g-PAM–silica/GCE ^b	-0.6 (SCE ^k)	1–3900	26	0.06	24
NPC/GCE ^c	-0.62 (Ag/AgCl)	2–100	126	0.62	25
PNMPC/Nafion/GCE ^d	-0.7 (Ag/AgCl)	1–200	6.93	0.05	26
MMPCM ^e /GCE	-0.64 (SCE)	0.2–40	2360	0.008	27
BiF/CPE ^f	-0.65 (SCE)	1–100	289	0.83	28
OMC/DDAB/GCE ^g	-0.5 (Ag/AgCl)	20–2900	-	10	29
EAG/SPCE ^h	-0.624 (Ag/AgCl)	0.3–374.5	102.6	0.06	30
SiO ₂ /Au NPs/GCE ⁱ	-0.74 (Ag/AgCl)	0.1–25	102	0.1	31
HMDE ^j	-0.8 (Ag/AgCl)	14.7–1000	-	5	32
Pd@POMs/MPC-2–GCE	-0.59 (Ag/AgCl)	1–70 70–1000	943.3 706.8	0.42	This work

a Silver nanoparticles decorated reduced graphene oxide modified glassy carbon electrode

b Palladium nanoparticles decorated guar gum grafted polyacrylamide polymer-silica nanocomposite modified glassy carbon electrode

c Nitrogen doped porous carbon modified glassy carbon electrode

d Pt nanoparticles ensemble on macroporous carbon hybrid nanocomposites/Nafion modified glassy carbon electrode

e Macro-/meso-porous carbon materials were modified on the surface of a glassy carbon electrode

f A bismuth-film modified carbon paste electrode

g Ordered mesoporous carbon/didodecyldimethylammonium bromide composites film coated glassy carbon electrode

h Electrochemically activated graphite modified screen printed carbon electrode

i Silica-stabilized gold nanoparticles modified glassy carbon electrode

j Hanging mercury drop electrode

k Saturated calomel electrode

Table S6 Comparison of responses of Pd@POMs/MPC-1, 2, and 3-GCE to hydrazine, H₂O₂, and NB

Samples	Electrode	Peak potential (V)	Peak current (μ A)
hydrazine	Pd@POMs/MPC-1-GCE	-0.09	23.51
	Pd@POMs/MPC-2-GCE	0	46.68
	Pd@POMs/MPC-3-GCE	-0.04	38.55
H_2O_2	Pd@POMs/MPC-1-GCE	-0.23	51.37
	Pd@POMs/MPC-2-GCE	-0.17	58.42
	Pd@POMs/MPC-3-GCE	-0.21	53.49
NB	Pd@POMs/MPC-1-GCE	-0.70	76.74
	Pd@POMs/MPC-2-GCE	-0.59	130.33
	Pd@POMs/MPC-3-GCE	-0.61	102.26

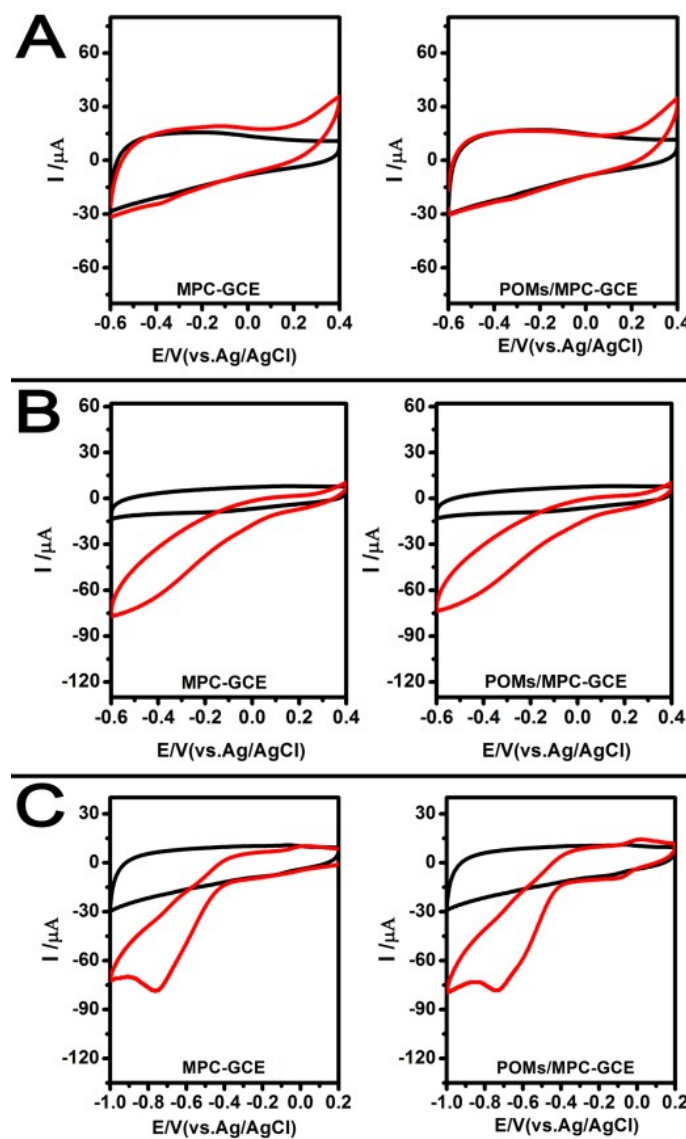


Fig. S9 CVs of POMs/MPC-GCE and MPC-GCE in the absence (black line) and presence (red line) of 100 μ M hydrazine (A), 1.0 mM H_2O_2 (B), and 100 μ M NB (C). Scan rate: 50 mV s⁻¹; pH=7.0.

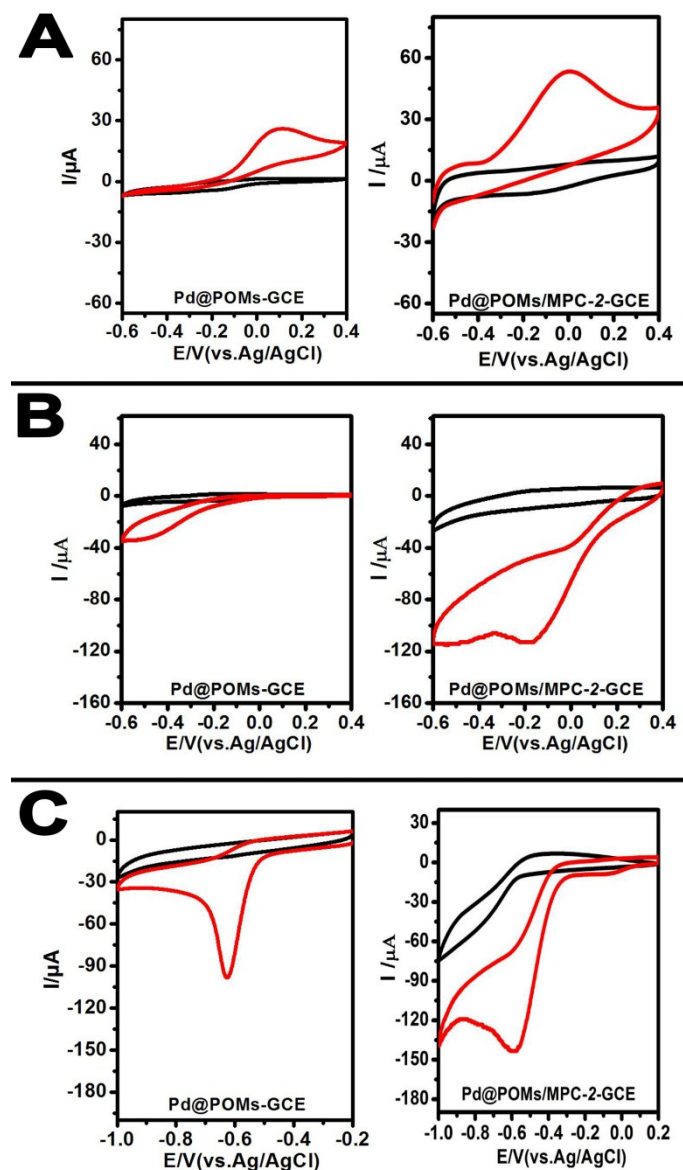


Fig. S10 CVs of Pd@POMs-GCE and Pd@POMs/MPC-2-GCE in the absence (black line) and presence (red line) of 100 μM hydrazine (A), 1.0 mM H_2O_2 (B), and 100 μM NB (C). Scan rate: 50 mV s^{-1} ; pH=7.0.

References

1. R. Madhu, B. Dinesh, S.-M. Chen, R. Saraswathi and V. Mani, *RSC Adv.*, 2015, **5**, 54379-54386.
2. R. S. Andre, A. Pavinatto, L. A. Mercante, E. C. Paris, L. H. C. Mattoso and D. S. Correa, *RSC Adv.*, 2015, **5**, 73875-73881.
3. A. Samadi-Maybodi, S. Ghasemi and H. Ghaffari-Rad, *Sens. Actuators, B*, 2015, **220**, 627-633.
4. J. Zhang, W. Gao, M. Dou, F. Wang, J. Liu, Z. Li and J. Ji, *Analyst*, 2015, **140**, 1686-1692.
5. S. P. Kim and H. C. Choi, *Sens. Actuators, B*, 2015, **207**, Part A, 424-429.
6. A. Ejaz, M. S. Ahmed and S. Jeon, *Sens. Actuators, B*, 2015, **221**, 1256-1263.
7. J. Zhang, H. Liu, M. Dou, F. Wang, J. Liu, Z. Li and J. Ji, *Electroanalysis*, 2015, **27**, 1188-1194.
8. A. A. Ensafi, M. M. Abarghoui and B. Rezaei, *Electrochim. Acta*, 2016, **190**, 199-207.
9. S. H. Kazemi, B. Hosseinzadeh and S. Zakavi, *Sens. Actuators, B*, 2015, **210**, 343-348.
10. A. R. Fakhari, H. Ahmar, H. Hosseini and S. Kazemi Movahed, *Sens. Actuators, B*, 2015, **213**, 82-91.
11. J. Zhao, J. Liu, S. Tricard, L. Wang, Y. Liang, L. Cao, J. Fang and W. Shen, *Electrochim. Acta*, 2015, **171**, 121-127.
12. A. A. Ensafi, M. M. Abarghoui and B. Rezaei, *Sens. Actuators, B*, 2014, **196**, 398-405.
13. J. Wang, H. Gao, F. Sun and C. Xu, *Sens. Actuators, B*, 2014, **191**, 612-618.
14. M. Baghayeri, E. Nazarzadeh Zare and M. Mansour Lakouraj, *Biosens. Bioelectron.*, 2014, **55**, 259-265.
15. C. Karuppiah, S. Palanisamy, S.-M. Chen, V. Veeramani and P. Periakaruppan, *Sens. Actuators, B*, 2014, **196**, 450-456.
16. H. Wu, S. Fan, X. Jin, H. Zhang, H. Chen, Z. Dai and X. Zou, *Anal. Chem.*, 2014, **86**, 6285-6290.

17. Y. Wang, Z. Wang, Y. Rui and M. Li, *Biosens. Bioelectron.*, 2015, **64**, 57-62.
18. J. Liu, X. Bo, Z. Zhao and L. Guo, *Biosens. Bioelectron.*, 2015, **74**, 71-77.
19. J. Ju and W. Chen, *Anal. Chem.*, 2015, **87**, 1903-1910.
20. L. Xing, Q. Rong and Z. Ma, *Sens. Actuators, B*, 2015, **221**, 242-247.
21. V. Mani, R. Devasenathipathy, S.-M. Chen, S.-F. Wang, P. Devi and Y. Tai, *Electrochim. Acta*, 2015, **176**, 804-810.
22. H. Kivrak, O. Alal and D. Atbas, *Electrochim. Acta*, 2015, **176**, 497-503.
23. C. Karuppiah, K. Muthupandi, S.-M. Chen, M. A. Ali, S. Palanisamy, A. Rajan, P. Prakash, F. M. A. Al-Hemaid and B.-S. Lou, *RSC Adv.*, 2015, **5**, 31139-31146.
24. P. K. Rastogi, V. Ganesan and S. Krishnamoorthi, *Electrochim. Acta*, 2014, **147**, 442-450.
25. L. Yan, X. Bo, Y. Zhang and L. Guo, *Electrochim. Acta*, 2014, **137**, 693-699.
26. Y. Zhang, L. Zeng, X. Bo, H. Wang and L. Guo, *Anal. Chim. Acta*, 2012, **752**, 45-52.
27. J. Ma, Y. Zhang, X. Zhang, G. Zhu, B. Liu and J. Chen, *Talanta*, 2012, **88**, 696-700.
28. L. Luo, X. Wang, Y. Ding, Q. Li, J. Jia and D. Deng, *Anal. Methods*, 2010, **2**, 1095-1100.
29. B. Qi, F. Lin, J. Bai, L. Liu and L. Guo, *Mater. Lett.*, 2008, **62**, 3670-3672.
30. B. Thirumalraj, S. Palanisamy and S. Chen, *Int. J. Electrochem. Sci.*, 2015, **10**, 4173-4182.
31. S. Singh, P. Devi, D. Singh, D. Jain and M. Singla, *Gold Bull.*, 2012, **45** (2), 75-81.
32. S. Liang, H. Zhang and D. Lu, *Environ. Monit. Assess.*, 2007, **129** (1-3), 331-337.